Cement and Concrete Research 40 (2010) 1060–1071

Contents lists available at ScienceDirect

Cement and Concrete Research

journal homepage: http://ees.elsevier.com/CEMCON/default.asp

Influence of the porosity gradient in cement paste matrix on the mechanical behavior of mortar

E. Herve [a,*], S. Care [b], J.P. Seguin [a]

[a] Laboratoire d'Ingénierie des Systèmes de Versailles, Université de Versailles, Saint-Quentin en Yvelines, 45 Avenue des Etats-Unis, F-78035 Versailles Cedex, France
[b] Université Paris-Est, UR Navier, UMR CNRS LCPC, 2 allée Kepler, 77420 Champs-sur-Marne, France

ARTICLE INFO

Article history:
Received 7 April 2008
Accepted 21 February 2010

Keywords:
Porosity
Mortar (E)
Mechanical behavior
Interfacial Transition Zone (B)
Micromechanical

ABSTRACT

This paper is devoted to the study of the influence of the microstructure of mortar on its mechanical behavior. For this purpose, mechanical tests have been carried out on mortars and a mathematical model, the $(n+1)$-phase model, has been used to take into account three variable parameters of the microstructure of mortar (the thickness of the interfacial transition zone, the porosity gradient in the cement paste matrix and the nature of the constituents of the Interfacial Transition Zone) for some given parameters (volume fraction of aggregates, porosity of the mortar and mechanical behavior of the aggregates and the cement paste). By fitting some measured moduli to the model predictions, we can estimate in a non-destructive manner, the possible distribution of porosity within the Interfacial Transition Zone. Our results provide information on the data such micromechanical models can deal with in order to predict the elastic behavior of mortars.

© 2010 Elsevier Ltd. All rights reserved.

1. Introduction

1.1. Background

The earliest and simplest models used to predict the elastic moduli of cementitious materials were based on the assumption that concrete (or mortar) was made of two phases: aggregate (or sand) particles and cement paste. Under this assumption several models have been used in literature accounting or not for the fact that the cement paste is the connected phase whereas the inclusions form a disconnected dispersed phase (Zimmerman et al. [1] used the Kuster-TоksÃűz theory [2], Yang and Huang [3] or Bernard et al. [4] used the Mori–Tanaka theory [5], Nilsen and Monteiro [6] used Hashin–Shtrikman variational approach [7]). But as mentioned by Bernard et al. [4], the predicted elastic moduli may be overestimated with the assumption that concrete are considered to be made of two phases (aggregate and cement paste).

Indeed, it has become recognized that the cement paste should not be considered to be a homogeneous phase and the structure of the cement paste in the vicinity of the inclusions differs from that of bulk cement paste (Mehta and Monteiro [8] and Mindness [9]). This region in which the presence of the inclusions affects the properties of the cement paste is known as the Interfacial Transition Zone (ITZ) (this phenomena, due to a limitation in the packing of cement particles in the vicinity of aggregates is often referred to as the "wall effect"). The effective elastic properties of cementitious composites with an ITZ considered as a single phase with homogeneous properties have been extensively studied with different models. Yang [10] has proposed a double-inclusion model, Ramesh et al. [11], Li et al. [12,13] have used a four-phase sphere model which is an extension of Christensen and Lo's three-phase sphere model, Hashin and Monteiro [14] have used this four-phase model in an inverse manner to determine the elastic properties of the interphase, Sun et al. [15] have used the differential effective medium theory and numerical simulation.

In the ITZ, the porosity is greatest near the inclusions, and decreases with increasing distance from the inclusion leading to gradients of the elastic properties within this zone. In the case of dilute suspensions of aggregates Lutz and Zimmerman [16] (using power-law variation) and Garboczi and Bentz [17] (using piecewise variation) have taken into account those gradients. Nadeau [18,19] has developed a model of concrete elastic moduli which takes into account the gradient of properties in the ITZ. For that purpose, the local cement volume fraction through the ITZ is taken to vary in a quadratic manner. The parameters of the used quadratic law have been determined by requiring the conservation of the total amount of cement in the cement paste matrix to be that given by the mix design. These parameters depend upon the aggregate radius, the volume fraction of the aggregate, the specific gravity of cement and the thickness of ITZ.

1.2. Notations

The mortars are here considered as composite materials made of three phases (as simplified in Fig. 1):

- let phase A denote the aggregate phase with an average radius denoted R_A and with homogeneous mechanical properties,

* Corresponding author.
E-mail address: eveline.herve@meca.uvsq.fr (E. Herve).

0008-8846/$ – see front matter © 2010 Elsevier Ltd. All rights reserved.
doi:10.1016/j.cemconres.2010.02.010

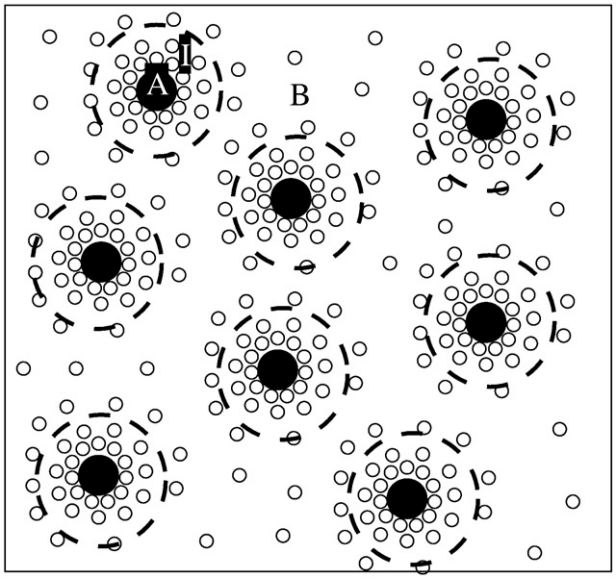

Fig. 1. Mortar representation with phase A: aggregate, phase I: ITZ characterized by a dotted line and phase B: bulk cement paste. Porosity gradient in cement paste matrix (ITZ + bulk cement paste matrix) is simulated by small circles.

- let phase I denote the ITZ phase with an average thickness t_I and characterized by a porosity gradient leading consequently to a gradient of mechanical properties,
- and let phase B denote the bulk cement paste characterized by the cement paste which is "globaly" homogeneous (its porosity is distributed in a homogeneous manner) with homogeneous mechanical properties.

Let f_A, f_I and f_B be respectively the volume fractions of phase A, phase I and phase B. The ITZ I and the bulk cement paste B constitute the cement paste matrix.

1.3. Aim of the paper

The present paper aims to bring informations on the parameters such micromechanical models can take into account to predict the elastic moduli of mortars and attempts to improve previous works by:

1. Taking the porosity through the ITZ to follow a power-law which is not necessary a linear or a quadratic one and which depends on two parameters (factor A and exponent m defined in Eq. (5)),
2. Considering the ITZ as a porous material, the matrix of what (M_I) being able to consist of different materials (portlandite (CH) or "Solid Phase" (*SPCP*) which is mainly made of anhydrous and hydrate phases such as CSH), the thickness of what (t_I) being able to be chosen,
3. Performing the determination of the mechanical behavior of the bulk cement paste B by using first a Generalized-Self-Consistent in an inverse manner to determine the mechanical behavior of the "Solid Phase" named SPCP from the experimental one of a cement paste and then in a direct manner by taking into account the porosity of this bulk cement paste (p_B). One of the parameters of the power-law (factor A) is found by requiring the total porosity p in each considered mortar to be that given by the mix design and the other (the exponent m) is determined by fitting the model predictions to some measured moduli. The identification of the gradient of properties of the cement paste matrix is determined from our own experimental results and also from literature results.

It is worth noting that the exponent m being limited by the fact that the porosity must be lower to one and to the maximum of the porosity in the ITZ being at the interface aggregate/ITZ, this model can also be used to deal with damage of mortar and more particularly with complete misfitting at the interface aggregate/ITZ.

2. Model development

2.1. Introduction

Let us consider mortars for which the volume fraction of each phase (f_A for the aggregate A, f_I for the ITZ I and f_B for the bulk cement matrix B), the global porosity of each phase (p_A for the aggregate A, p_I for the ITZ I and p_B for the bulk cement matrix B), the mechanical effective properties (Young's Modulus E, Poisson's coefficient ν) and their total porosity p are known. In order to predict the macroscopic properties, two levels of modeling were considered (referenced as levels II and III in [4]):

- Firstly, the elastic properties of the cement paste matrix (ITZ and bulk cement paste) have been determined thanks to the $(2+1)$-phase model from the porosity of the porous material and the elastic properties of the solid phase. The elastic properties of the solid phase can be found in literature (for instance in [31]) or can be determined thanks to a $(2+1)$-phase model used in an inverse mode from the elastic properties of a cement paste. The solid phase (labeled SPCP) determined from a cement paste was mainly composed of anhydrous cement and hydrate phases. The cement paste and the mortars have the same water to cement ratio.
- Secondly, the elastic properties of the mortar were determined using a $(n+1)$-phase model which allowed taking into account the porosity gradient in cement paste matrix (ITZ and bulk cement paste) and consequently the gradient of elastic properties.

2.2. (n + 1)-phase model

We have chosen to use here a Generalized-Self-Consistent Scheme because this kind of model is very well adapted to deal with every kind of inclusion/matrix composites. However, it is always necessary to take care to the way the experimental parameters of the studied materials are determined in order to be used in the model.

Let R_i, $i \in [1, n]$ be respectively the radius of the different spheres in the composite sphere in Fig. 2 by beginning the numbering from the

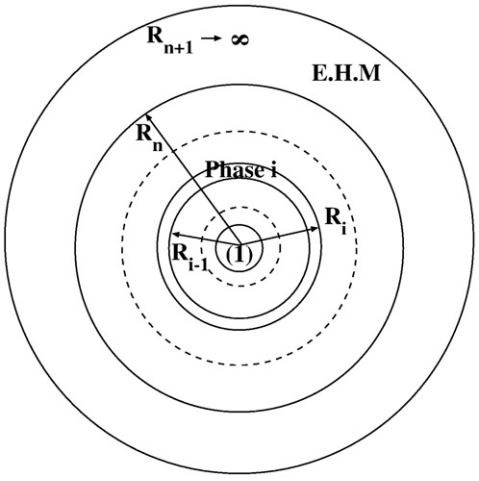

Fig. 2. The n-phase model.

center of the composite sphere. They are determined by the phase volume fractions only, through the relations:

$$\left(\frac{R_1}{R_n}\right)^3 = f_1, \left(\frac{R_i}{R_n}\right)^3 = f_1 + \ldots + f_i. \quad (1)$$

where f_i denotes the volume fraction of phase i. The effective moduli of the Equivalent Homogeneous Medium (E.H.M in Fig. 2), k^{eff} and μ^{eff}, are then determined straightforwardly from Eqs. (46) and (51) of Hervé and Zaoui [31], (or see in appendix Eqs. (20) and (21)).

The $(n+1)$-phase model can be used with $n=3$ in an inverse manner to determine the mechanical behavior of the ITZ when the behavior of the cement paste, the aggregates and the mortar are known likewise the radius of the aggregates and the thickness of the ITZ. In this case the properties of all the different phases are supposed to be homogeneous. The same data as Hashin and Monteiro [14] have been used here. This comparison shows that Hashin and Monteiro [14] have the same results as the $(n+1)$-phase model gives with $n=3$ [31].

Moreover the $(n+1)$-phase model can be used to deal with mortar with a gradient of properties in the cement paste matrix. This gradient of properties can also be determined thanks to the $(n+1)$-phase model used in an inverse mode. The procedure is described hereafter.

2.3. Different distributions of porosity

The distribution of porosity in the cement paste matrix has to be determined. For that purpose, a new methodology has been developed from the total porosity p.

In this section, the total porosity in the mortar (p) can be distributed in several manners. If $p_I(r)$ denotes the local porosity in spherical coordinates (r, θ, ϕ), by requiring the total porosity in the mortar to be that given by the experimental measurements (cf Table 1) whatever the distribution of porosity is, it follows that:

$$\iiint_{V_{\text{total}}} p_I(r)dc(r) = p \quad (2)$$

where $dc(r)$ denotes the volume fraction of material between radii r and $r+dr$. This equation can also be rewritten under the following form:

$$\frac{1}{V_{\text{total}}}\iiint_{V_{\text{total}}} p_I(r)dV = p \quad (3)$$

Using the $(n+1)$-phase model, all the phases lay inside the composite sphere with radius R_n (Fig. 2). A normalized distance to the center of the aggregate is then defined by $x = \frac{r}{R_n}$ with $x_A = f_A^{1/3}$, $x_I = (f_A+f_I)^{1/3}$, $x_B = 1$. According to this new variable, Eq. (3) reads now:

$$3\int_0^1 p_I(x)x^2dx = p \quad (4)$$

Table 1
Experimental data on material proportions. W/C: water to cement ratio, f_A: aggregate volume fraction of sand, $D_{\min}/D_{\max}$: lower and upper diameter of sand, R_A: average radius of sand for 50% passing, A_b: absorption coefficient of sand, f_I: Interfacial Transition Zone volume fraction, t_I: thickness of ITZ according to Eq. (10).

Material	p	MC	MM	MF
W/C	0.45	0.45	0.45	0.45
f_A(%)	/	0.5	0.5	0.5
$D_{\min}/D_{\max}$(mm)	/	2/4	0.315/2	0.315/1
R_A (mm)	/	1.2	0.5	0.35
A_b (%)	/	0.058	0.405	0.1
f_I (%), $t_I=30$ μm	/	3.6	10.3	15.4
f_I (%), $t_I=60$ μm	/	7.4	20.8	29.8

In this paper, a power-law function defined by two parameters (A and the exponent m) has been used to model the distribution of porosity in the ITZ I, the porosity in the bulk cement paste B has been chosen constant equal to p_B (p_B has different possible values in the applications) and in all the studied cases the aggregates A are porousless:

$$p(x) = \begin{array}{ll} p(x)=0 & x\in[0,x_A] \\ p(x)=A(x_I-x)^m+p_B & x\in[x_A,x_I] \\ p(x)=p_B & x\in[x_I,1] \end{array} \quad (5)$$

The first parameter of the model (A) is obtained by taking into account Eq. (4) with the distribution of porosity defined by Eq. (5) and is given by:

$$A = \frac{p-p_B\left(1-x_A^3\right)}{3I_m} \quad (6)$$

with

$$I_m = \frac{(x_I-x_A)^{m+1}}{(m+1)(m+2)(m+3)}\left[(m+2)(m+3)x_A^2 + 2(m+3)x_A(x_I-x_A) + 2(x_I-x_A)^2\right] \quad (7)$$

The second parameter of the model (the exponent m) is then determined by requiring the effective Young's modulus of the studied mortar to be the experimental one. Different values of m can be found. It is worth noting that:

1. for $m=0$, $p_I(x)$ is constant both in the ITZ I and in the bulk cement paste B as considered in [4]. If $p_I(x)=\alpha$ in the ITZ and $p_I(x)=\beta$ in the matrix, Eq. (4) leads to the fact that it exists d so that:
$$p_I = \alpha = \frac{dp}{f_I} \text{ and } p_B = \frac{(1-d)p}{f_B} \quad (8)$$
where the physical meaning of d is the ratio between the volume of pores in the ITZ and the whole volume of pores. $1-d$ is then the ratio between the volume of pores in the bulk cement paste and the whole volume of pores in the cement paste matrix.
2. $m=1$ corresponds to a “linear distribution”
3. $m=2$ corresponds to a “quadratic distribution”, as considered in Nadeau ([18] and [19]).

It is worth noting that, to avoid local porosity greater than one, the maximum porosity ($p_{\max}$) of mortar has to be lower than one:

$$p_{\max} = \left[A(x_I-x_A)^m + p_B\right] \le 1 \quad (9)$$

This restriction leads to a maximum value for m.

2.4. Applications to mortars with a porosity gradient

The aggregates are poreless, the ITZ is made of a porous material (which the matrix has been chosen to be either Porlandite or “SPCP”) with the porosity defined by Eq. (5) and the bulk cement paste B has been considered as a porous material with the porosity p_B and with the material “SPCP” as solid matrix. The porosity gradient inside the mortar is determined from experimental data obtained from mortars and cement pastes with the same water to cement ratio. The knowledge of the porosities of the different phases is required (Fig. 3).

In order to use the $(n+1)$-phase model the following discretization is applied:

- Phase 1: aggregate
- Phase 2 to $n-1$: different layers in the ITZ
- Phase n: bulk cement paste
- Phase $n+1$: Equivalent Homogeneous Medium

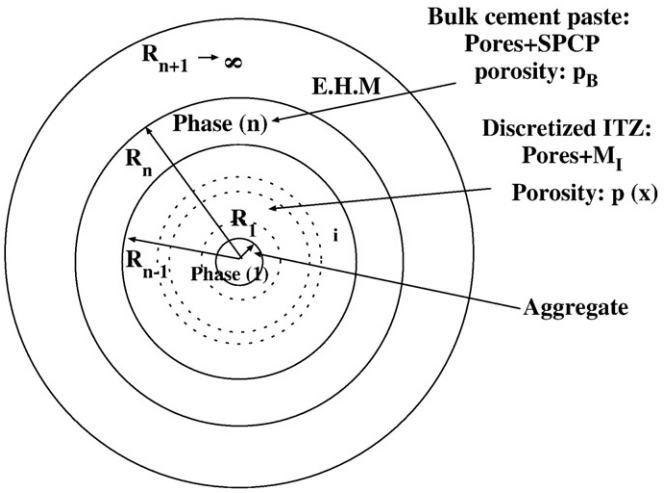

Fig. 3. Adaptation of the $(n+1)$-phase model to mortar.

The different steps of the application of the $(n+1)$-phase model are then:

1. Determination of the parameter A as a function of the parameter m from the experimental data (f_A, t_I, p and p_B) according to Eq. (6).
2. Determination of the behavior of the "SPCP" phase thanks to an inverse $(2+1)$-phase model (adapted to porous materials Eqs. (16) and (21) from the measured moduli of the cement paste.
3. Determination of the behavior of the bulk cement paste with Eqs. (16) and (15) used in a direct manner with the porosity p_B and the matrix "SPCP".
4. Choice of the solid phase of the ITZ (here portlandite or "SPCP").
5. Determination of the global behavior as a function of m.
6. Determination of the possible distribution of porosity within the Interfacial Transition Zone (different possible values of m) by fitting the model predictions to the measured moduli (here either for a given value of m the effective behavior of the mortar is determined, or for a given Young's modulus of a mortar the corresponding value of m is performed).

In Section 3, experimental results are presented. Mortars are cast with different aggregate sizes to study the sand size effect. A procedure allowing the determination of global porosities of the different phases (and more particularly in the ITZ phase) is proposed.

In Section 4 the model development is applied. Input data are discussed through parameter studies.

3. Experimental study

In order to study the effect of ITZ on the mechanical properties of mortars and to determine the relevant input data used by the micromechanical model, experimental tests have been performed, on the one hand on mortars denoted M with different aggregate size and with the same aggregate volume content and on the other hand, on one cement paste denoted CP. This test program allows us to characterize the influence of the porosity gradient in cement paste matrix on the macroscopic properties as shown, for instance, in Caré [20] and Caré and Hervé [21] for the diffusive properties.

3.1. Material and specimen preparation

Four types of materials have been tested: a cement paste (denoted CP) and three types of mortars (denoted MC, MM and MF) with the same water to cement ratio (W/C = 0.45). The cementitious materials are made of Portland cement (European grade CEM I, 52.5), with a specific Blaine surface area of 3200 cm^2/g and with an average cement diameter of about 30 μm (Fig. 4). The mortars M have been cast with three types of round sand: the first one was a fine siliceous sand (0.315/1 mm) labeled F, the second one was a medium siliceous sand (0.315/2 mm) labeled M and the third one was a coarse siliceous sand (2/4 mm) labeled C. Fig. 5 shows the grain size distribution of these sands. They are considered as non porous because their absorption coefficients are lower than 0.5%. The sand volume fraction f_A was equal to 0.50. A superplasticizer was used to minimize air void content.

After mixing, the mixes were poured in cylindrical moulds (Φ 70×150 mm) without vibration to avoid segregation. A rotating set up was used for 24 h during setting to obtain homogeneous samples without segregation. After demoulding, specimens were tightly wrapped in two superimposed adhesive aluminum sheets until the beginning of experiments.

3.2. Microstructure analysis

The microstructure of the studied materials has been investigated by Mercury Intrusion Porosimetry (MIP) measurements and by Scanning Electron Microscopy (SEM) observations. Before testing, the samples have been dried by a freeze-drying technique. The details of the experimental procedures are given in Caré [20] and the main results are summarized hereafter.

3.2.1. SEM analyses and volume fraction of ITZ

Details of the spatial distribution of the different phases (A, I or B) and then of the porosity are given in Figs. 6–8 from SEM observations. A layer characterized by a darker ring was observed at the interface aggregate/cement paste for all the mortars (Figs. 6.1 and 7). This layer characterizes the ITZ phase. Our observations showed that ITZ features are highly variable from location to location (Fig. 7). Its measured thickness t_I ranged between 0 and about 60 μm (as seen in Fig. 7). A mean value around 30 μm is considered as the average

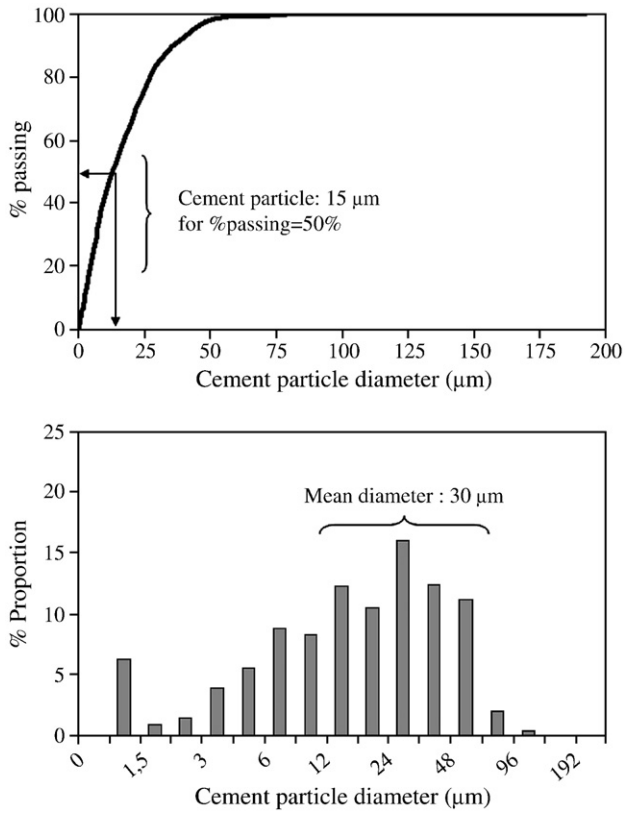

Fig. 4. Grain size distribution of the used cement.

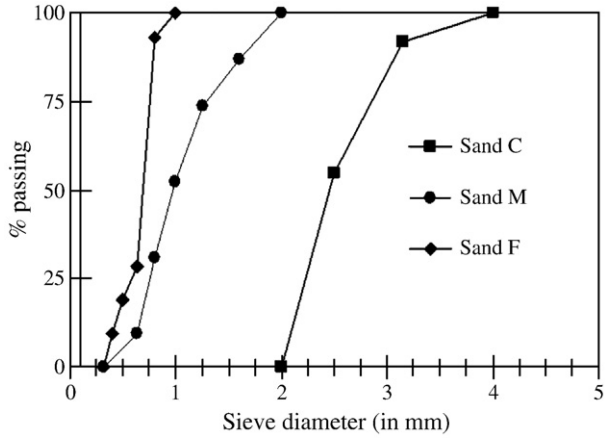

Fig. 5. Grain size distribution for the sand C (2/4 mm) M (0.315/2 mm) or F (0.315/1 mm).

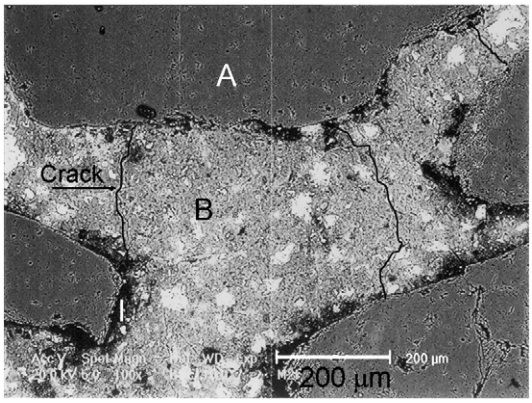

Fig. 7. SEM observations on polished surface for mortar MF with aggregates A, ITZ I and bulk cement paste B. ITZ phase: darker ring variable thickness (0–60 µm).

thickness of the ITZ and corresponds to about the median size of cement grains (or twice the size of cement grains for a passing equal to 50%, Fig. 4).

Furthermore the ITZ phase appears as an inhomogeneous phase with large detectable porosity (Figs. 6.3 and 8) and dense material (with a high amount of portlandite). According to previous works [22], there is a porosity gradient in the ITZ phase which depends on the composition of the ITZ phase. For instance, SEM observations coupled with EDS analysis (Fig. 8) show that large crystals of portlandite (CH) are sometimes deposited on aggregate particles so that the porosity in the layer close to the aggregate may be very low. Some ettringite can be observed in the ITZ phase (Fig. 6.3) as mentioned by Monteiro and Mehta [23] but in smaller proportion.

Generally the ITZ zone is very porous within the first µm from the aggregates surface.

Furthermore, as shown by Scrivener [24], it is difficult to exhibit an "average" ITZ microstructure because there are large variations of microstructure in the ITZ. Even if the visual observations of the ITZ features look like for all mortars, the distribution of porosity versus the distance from the aggregate is different for coarse and small aggregates according to Basheer et al. [25].

Far from the ITZ zone a denser material can be observed with homogeneous properties. The microstructure in the bulk cement paste (Fig. 6.4) is quite dense and without a large porosity. This phase is mainly composed of a C–S–H products and anhydrous cement.

The ITZ volume content f_I according to Garboczi [17] is given by:

$$f_I = 1 - e_V(t_I) - f_A, \tag{10}$$

This equation takes into account the overlaps of the interfacial transition zones. The functional form of $e_V(r)$ is given by:

$$e_V(r) = (1 - f_A)e^{-\pi\rho(cr + dr^2 + gr^3)}, \tag{11}$$

where ρ is the total number of aggregates per unit volume, r is the thickness of a spherical shell added around each one of aggregate spherical particle, and the coefficients c, d, and g are given in term of average over the aggregate particle size distribution. The function $e_V(r)$

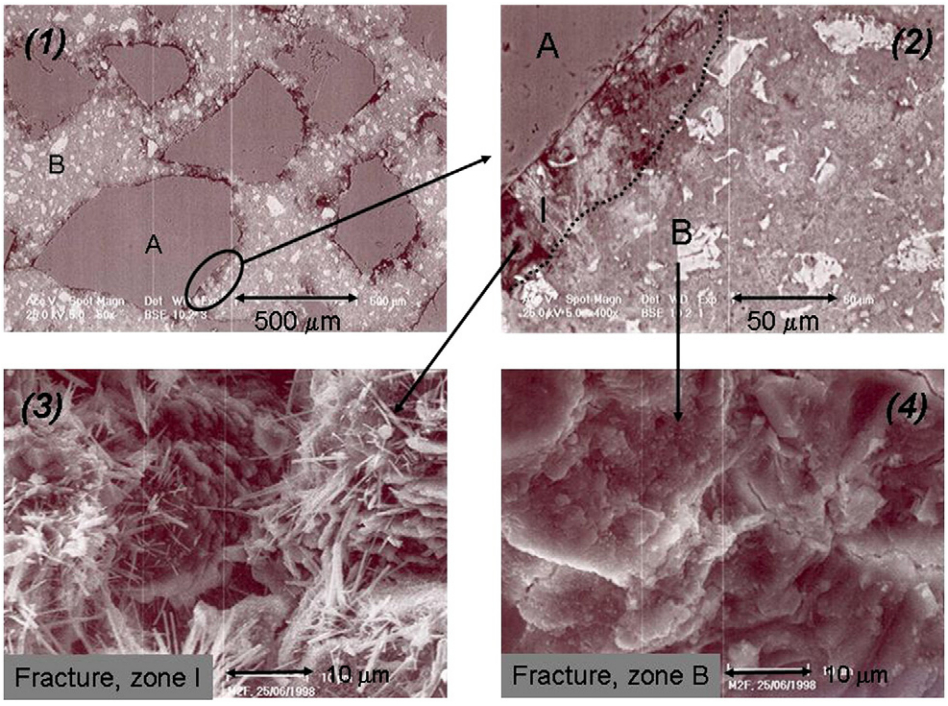

Fig. 6. SEM observations for mortar MF with phases A = aggregate, I = ITZ and B = bulk cement paste. (5.1, 5.2): observations on polished surface; (5.3, 5.4): examples of ITZ and bulk cement paste on fracture surface.

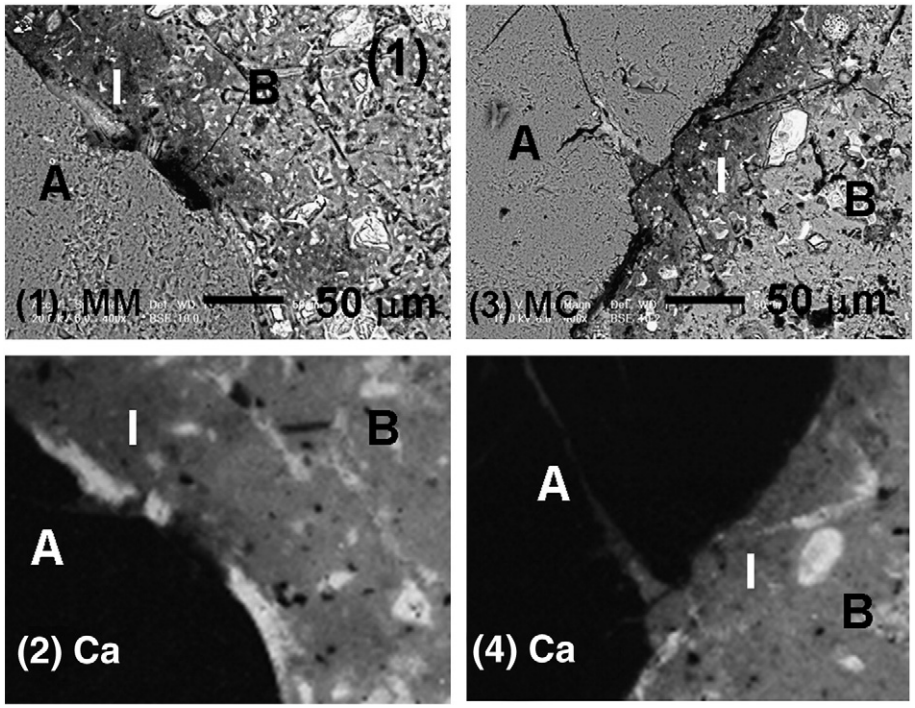

Fig. 8. SEM observations for mortar MM (8.1) and MC (8.3) and element Ca repartition by EDS at the interface sand/cement paste for mortars MM (8.2) and MC (8.4). White zone represents phase with high level of calcium. With phases A = sand, I = ITZ and B = bulk cement paste.

is determined from the volume fraction of aggregates, the aggregate size distribution, which is given in Fig. 5, and the thickness of ITZ ($r = t_I$). Table 1 gives the values of f_I for each mortar for $t_I = 30$ µm or $t_I = 60$ µm.

3.2.2. Pore size distribution

Mercury Intrusion Porosimetry (MIP) measurements have been carried out to determine the pore size distribution. For each specimen, three samples have been tested and the results averaged. Fig. 9 presents the pore size distribution of the mortars (MC, MM, MF) and of the cement paste CP (given for the same mass of cement paste matrix). The porosity characteristics for each mixture are summarized in Table 2.

The presence of aggregates A tends to modify the pore structure of the materials. On the one hand, the distribution of hydrate pores ($R_p \simeq 20$ nm) is slightly shifted towards finer pores and the proportion of this kind of pores in mortars is lower than the one of the cement paste CP. On the other hand, coarse pores ($R_p > 200$nm) appear and are attributed to the presence of the ITZ phase I located at the interface sand/cement paste. These results are in accordance with previous published results [26] showing that porous ITZ are expected to be accompanied with more dense bulk cement pastes, i.e. less porous bulk cement paste (with respect to the water-cement ratio).

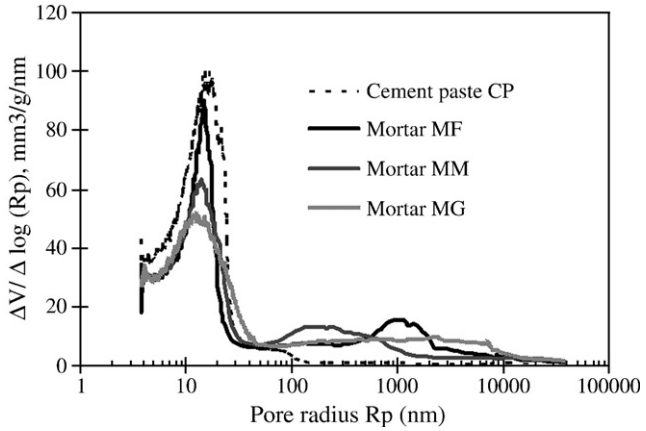

Fig. 9. Incremental porosity versus pore radius R_P (nm) for mortars MC, MM, MF and cement paste P (for the same mass of cement paste matrix).

3.2.3. Determination of the global porosity in the different phases

The model development for determining the porosity gradient in the cement paste matrix (Eq. (6)) requires having the global porosity in the different phases. For that purpose, MIP measurements are used assuming that the increase of porosity may be attributed to the ITZ phase.

The proportion of pores with a radius lower than 200 nm is attributed to the porosity of bulk cement paste B in mortars because the proportion of the porosity >200 nm for the cement paste CP is inferior to 3% (see Table 2) and because the ITZ layers around the aggregates A are interconnected thanks to cracking generated by autogeneous shrinkage or by drying shrinkage due to freeze-drying (Fig. 7). So, it may be considered that all the volume of mercury above 200 nm corresponds to the ITZ porosity and that all the volume of mercury under 200 nm corresponds to the bulk cement paste porosity. The porosity named p_B in phase B is:

$$p_B = p_P * A_B / A_P \quad (12)$$

where p_B (%) is the porosity of bulk cement paste B in mortars, p_P (%) is the porosity of the cement paste CP, A_B (%) and A_P (%) are the proportion

Table 2
Experimental data on porosity characteristics: mercury porosity characteristics: total porosity P (%), relative proportion in % of hydrates porosity ($R_p < 200$ nm) and of capillaries pores ($R_p > 200$ nm). Average porosity in the bulk cement paste p_B and in the ITZ p_I according to Eqs. (12) and (13).

Material	p	MC	MM	MF
Total porosity p(%)	22.6	11	12.2	13
% small pores ($R_P < 200$ nm)	97.4	69.7	77.7	78.2
% capillaries pores ($R_P > 200$ nm)	2.6	30.3	22.30	21.8
p_B (%)	22.6	16.2	18	18.2
p_I (%) with $t_I = 30$ µm	/	97.1	49	43.7
p_I (%) with $t_I = 60$ µm	/	55.6	33.4	31.3

of pores in mortars M and cement paste P with a radius lower than 200 nm.

Moreover, the average porosity in ITZ phase p_I for all the ITZ thicknesses t_I may be estimated according to (see Table 2):

$$p = f_I p_I + f_B p_B \quad (13)$$

It appears that the porosity in the bulk cement paste p_B is all the more important as the sand is fine. Furthermore, the coarser the aggregates are, the more porous it is at the ITZ as a consequence of lower porosity in the bulk cement paste (Table 2). This result means that the large aggregate particles tend to accumulate more bleed water around it than smaller aggregate particles so that the local water-cement ratio in the bulk cement paste or the porosity in the bulk cement paste are lower for large aggregate particles than for smaller ones. It can be noticed that the finer sand has a larger surface area (for the same volume content), so that an opposite effect could be expected: more bleed water on the fine sand. Our result, which is in accordance with Elshrief et al.'s results [27] showing that the ITZ porosity is lower with small aggregates, may be explained by the fact that the "intensity of the wall effect" depends upon the sand size.

Furthermore, it can be noticed that there are inherent problems associated with the MIP method, as mentioned by Diamond [28], which can lead to errors on the determination of the global porosity of the ITZ p_I and of the bulk cement paste p_B. Parametric study in Section 4 will be carried out to take into account this effect.

3.3. Elastic properties

Compressive strength tests on the specimen were performed on a MTS servo-hydraulic testing machine of 100 kN capacity at an imposed stress rate of 0.5 MPa/s on cylindrical specimen with a diameter of 70 mm, and height of 150 mm. For the determinations of Young's modulus and Poisson's coefficient a special extensometer, the J2P [29] was used. This extensometer consists of three displacement transducers (LVDTs) arranged at 120° to measure Young's modulus and of three displacement transducers diametrically placed to measure Poisson's coefficient. The displacement transducers are supported by aluminum rings in contact with the specimen through elastic heads.

The elastic properties for the cement paste CP and the mortars (MC, MM, MF) are given in Table 3. For each specimen, six samples have been tested and the results averaged. It is worth noting that the relative error on Young's modulus, between the average value (E_a) and the maximum or the minimum measured value (E_{min} or E_{max}) is lower than 6% for all the materials.

From data in Table 3, it can be seen that the modulus of elasticity increases with ITZ volume fraction f_I and that Poisson's ratio is quite similar whatever the size of sand.

Although the differences between the experimental moduli are weak, the effect of sand size is noteworthy and Young's moduli slightly increase with finer sand. The results for mortars MM and MF are the same order of magnitude because the grain size distributions of the sand M and the sand F are similar. Young's modulus for mortar MC is quite different in coherence with the grain size distribution. Furthermore measured Young's modulus may be correlated to the porosity p_I in the ITZ phase; it is all the more important as the porosity p_I in the ITZ phase is low.

Table 3
Experimental elastic properties. Young's modulus E, Poisson's ratio ν.

	E_{min}	Average E (GPa)	E_{max}	Average ν
P	16.1	16.54	17.3	0.23
MC	28.7	30.1	31.7	0.20
MM	31.5	32.8	33.0	0.19
MF	32.0	33.9	34.8	0.21

4. Relevant parameters influencing elastic properties

This section aims to determine which relevant microstructural parameters influence the elastic properties of mortars. The input parameters are presented hereafter, either given from our results (Section 3) or from literature results. The influence of those input parameters are discussed.

4.1. Input parameters

The input data for the three phases (A, I and B) are given as follows (Table 4):

- For the sand (A) with $f_A = 0.5$. As the mechanical properties of round sands are not well known, two types of mechanical properties have been considered:
  1. the first case corresponds to $E_A = 86.9$ GPa and $\nu_A = 0.17$ which are data considered in previous works [14,18,19] to study the influence of ITZ on mechanical behavior of mortars.
  2. the second case corresponds to $E_A = 70$ GPa with the assumption that $\nu_A = 0.2$.
- For the bulk cement paste (B) assumed to be composed mainly of "SPCP":
  - it was assumed that the elastic properties of the solid phase are the same as the ones of the cement paste CP. Applying step 2 presented in Section 4 we found for this material $E_{SPCP} = 26.61$ GPa, $\nu_{SPCP} = 0.233$. The values we get are the same order of magnitude than the values for the C–S–H (for instance in [4,30]).
  - the decrease of the porosity (labeled p_B) in the bulk cement paste compared to the porosity of the cement paste P has been here taken into account. The porosity p_B is determined from MIP tests according to Eq. (12). This point will be discussed after summarizing the main obtained results to take into account the inherent problems associated to MIP measurements.
- For the ITZ
  1. It can be noticed that the thickness is not constant around each aggregate but nevertheless it makes sense to consider a constant one in the model because the used model is based on average operation on the all the aggregates present in the mortar. Consequently, we have considered that the thickness of the many ITZ regions was uniform and then could be defined by the median cement particle diameter ($t_I = 30$ μm). Furthermore another case has been considered with ($t_I = 60$ μm) to take into account the heterogeneity of the thickness. The case without ITZ ($t_I = 0$ μm) is also considered in the discussion (see Table 5).
  2. Two cases for the mechanical properties of the solid phase have been considered:
     (a) The first mechanical properties of the solid phase we have considered here (named M_1) has been chosen equal to those of CH given in [4] assuming that the solid phase is mainly composed of CH ($E = 42.33$ GPa and $\nu = 0.324$).
     (b) The second ones (material named M_2) are those of the solid phase SPCP assuming that the solid phase is mainly composed of the solid phase SPCP (as in the bulk cement phase).

All these assumptions allowed studying whose parameters may affect the macroscopic properties.

Table 4
Mechanicals properties of the different phases.

Material	E GPa	ν
A_1	86.9	0.17
A_2	70	0.2
M_1	42.3	0.324
M_2	26.6	0.233

Table 5
Different thicknesses of the ITZ.

Thickness (t_I) of the ITZ	μm
t_1	30
t_2	60

4.2. Effect of the gradient of porosity in the ITZ phase

In order to understand the influence of the distribution of porosity in the ITZ on the mechanical properties of mortars, the effective Young's modulus versus the exponent m (see Section 3) has been determined for the mortar MF, taking into account the decrease of porosity in the bulk cement paste. The porosity p_B in the bulk cement paste and the total porosity p have been determined from MIP tests. In these applications, it is assumed that the ITZ is mainly composed of portlandite (CH) with a thickness equal to 30 or 60 μm. The effective Young's modulus versus the exponent m is given in Fig. 10. The effective Young's modulus decreases with the exponent m for all the cases. The upper and lower values of the exponent m may be determined from the maximum and the minimum measured Young's moduli. For example for the case (A_1, t_2, M_1), the exponent m ranges between 3.71 and 4.25 and is equal to 3.94 when the effective Young's modulus is equal to the average experimental value.

For all the cases, this result shows that the exponent m of the power-law depends on several parameters (thickness of the ITZ, mechanical properties of the sand) and cannot be a priori chosen (for instance constant, linear or quadratic distribution are not always possible).

4.3. Effect of the composition of the ITZ phase

In order to know which kind of composition of the ITZ (portlandite or "SPCP") can lead to an acceptable global Young's modulus, simulations have been carried out (see Tables 6–8) for different possibilities of the input parameters (aggregate, thickness of ITZ). Firstly the effective Young's modulus $E_{m=0}$ for the exponent m equal to zero (meaning that the ITZ is homogeneous) has been determined. Secondly, the exponent m which allows fitting the experimental average Young's modulus has been determined when the modulus $E_{m=0}$ is greater than it.

It is then possible to determine which parameters may affect the mechanical properties.

- If the effective Young's modulus $E_{m=0}$ for $m=0$ is lower than the minimum experimental Young's modulus, the input parameters cannot be used to estimate the mechanical properties ("NO" in the last column of Tables 6–8).

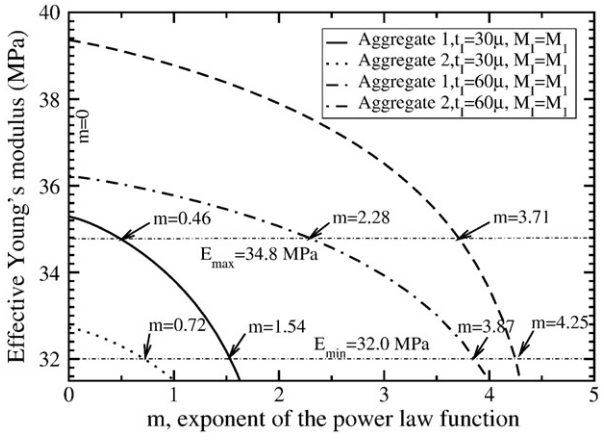

Fig. 10. Effective Young's moduli for the mortar MF and for different gradients of porosity.

Table 6
Effective behavior of the mortar MF for homogeneous ITZ ($m=0$) and exponent m fitting experimental Young's modulus.

A	t_I	M_I	$E_{m=0}$ (MPa)	$\nu_{m=0}$	m for $E^{eff}=33.9$ (MPa)	Possible
1	1	1	35.29	0.217	0.966	Yes
1	1	2	30.71	0.207	/	No
1	2	1	39.36	0.226	3.94	Yes
1	2	2	31.88	0.205	/	No
2	1	1	32.72	0.226	/	Partially
2	1	2	28.78	0.215	/	No
2	2	1	36.23	0.236	3.019	Yes
2	2	2	29.76	0.214	/	No

- If the effective Young's modulus $E_{m=0}$ for $m=0$ is greater than the minimum experimental Young's modulus there are two possibilities:
  1. $E_{m=0}$ is also greater than the maximum experimental Young's modulus, then the input parameters are acceptable ("Yes" in the last column of Tables 6–8).
  2. $E_{m=0}$ is lower than the maximum experimental Young's modulus, then the input parameters are partially acceptable ("Partially" in the last column of Tables 6–8).

These results show that the portlandite phase is always acceptable whatever the other input parameters are for MM and MF mortars. On the contrary, for the MC mortar, this conclusion is also "valid" for $t_I=60$ μm but not for $t_I=30$ μm because for this thickness the porosity is too high in the ITZ (see Table 2, $p_I=97.1\%$). It can be noticed that Poisson's ratio is quite similar whatever the input parameters.

4.4. Discussion

It is worth noting that the effective mechanical properties of mortars can also be predicted by a $(2+1)$-phase model (only taking into account the presence of aggregates and of a homogeneous cement paste). In this case the mechanical properties of the cement paste are considered to be equal to those of the cement paste CP.

The predicted effective Young's moduli E^{eff} are given for the mortars with the two sands A_1 and A_2 and compared to the experimental average

Table 7
Effective behavior of the mortar MM for homogeneous ITZ ($m=0$) and exponent m fitting experimental Young's modulus.

A	t_I	M_I	$E_{m=0}$ (MPa)	$\nu_{m=0}$	m for $E^{eff}=32.8$ (MPa)	Possible
1	1	1	34.66	0.214	0.946	Yes
1	1	2	31.07	0.207	/	No
1	2	1	38.01	0.219	3.51	Yes
1	2	2	32.48	0.205	/	Partially
2	1	1	32.19	0.223	/	Partially
2	1	2	29.12	0.215	/	No
2	2	1	35.06	0.290	2.819	Yes
2	2	2	30.31	0.214	/	No

Table 8
Effective behavior of the mortar MC for homogeneous ITZ ($m=0$) and exponent m fitting experimental Young's modulus.

A	t_I	M_I	$E_{m=0}$ (MPa)	$\nu_{m=0}$	m for $E^{eff}=30.1$ (MPa)	Possible
1	1	1	16.68	0.218	/	No
1	1	2	13.56	0.208	/	No
1	2	1	34.751	0.213	0.973	Yes
1	2	2	31.58	0.208	0.543	Partially
2	1	1	16.30	0.211	/	No
2	1	2	13.36	0.217	/	No
2	2	1	32.31	0.228	0.79	Yes
2	2	2	29.60	0.216	/	Partially

Table 9
Predicted Young's modulus E^{eff} with the $(2+1)$-phase model and relative errors between predicted values E^{eff} and experimental average ones E_a.

	Sand A_1	Sand A_2
E^{eff} (GPa)	34.14	31.72
$(E^{eff}-E_a)/E^{eff}$ for MC in %	11.75	5
$(E^{eff}-E_a)/E^{eff}$ for MM in %	3.7	−3.6
$(E^{eff}-E_a)/E^{eff}$ for MF in %	0.7	−6.8

value E_a by determining the relative error (see Table 9). For all the cases, the error is lower than 12%, which may be considered as suitable for the prediction of the mechanical properties because it is of the same order of magnitude than the experimental error. This $(2+1)$-phase model, on the contrary of the $(n+1)$-phase model, cannot be used to predict the possible composition of the ITZ (see Section 3) and is unable to predict the local porosity and mechanical properties in the cement paste. For the input parameters (A_1, t_2, M_1) which can be used for the three mortars, the local porosity and the local Young's modulus versus the normalized distance to the center of the aggregate (x defined in Section 3) are given in Figs. 11 and 12. Particularly these results show that the ITZ characteristics (porosity gradient and then gradient of mechanical properties) are different for small and coarse sands. It is important to take into account this porosity gradient, for instance, for the diffusion and leaching studies.

It is also worth noticing that these conclusions are linked to the used value of the porosity in the bulk cement paste (p_B), emphasizing the fact that it is necessary to get precise experimental results for p_B. The exponent m which allows fitting the experimental average Young's modulus has been determined for different porosity p_B of the bulk cement paste (Table 10).

Table 10 shows that, even for other values of p_B there is a porosity gradient in the ITZ and this gradient is always different with coarse and fine sands. Consequently, if there is an error in the experimental determination of p_B the kind of results would have been the same but with other values for m. It is worth emphasizing that the porosity in the bulk cement paste has to be different from the one of the cement paste CP, if not it would lead to a problem to determine the effective behavior of mortars with such porosity (see last line of Table 10).

5. Conclusion

The aim of this study was to determine which relevant microstructural parameters act on the effective elastic properties of mortars. For that purpose, a micromechanical model ($n+1$-phase) has been adapted to estimate in a non-destructive manner the possible distribution of porosity within the Interfacial Transition Zone and

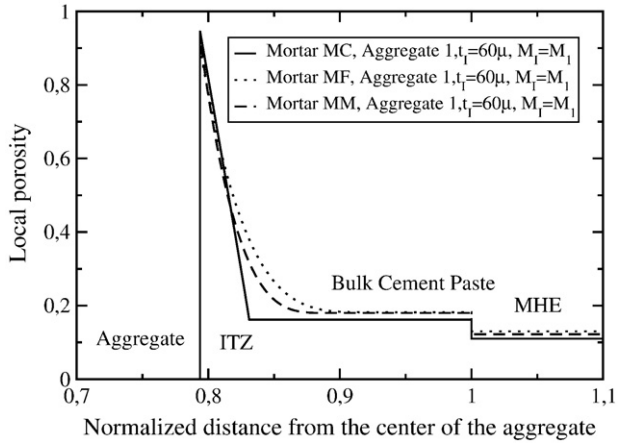

Fig. 11. Local porosity.

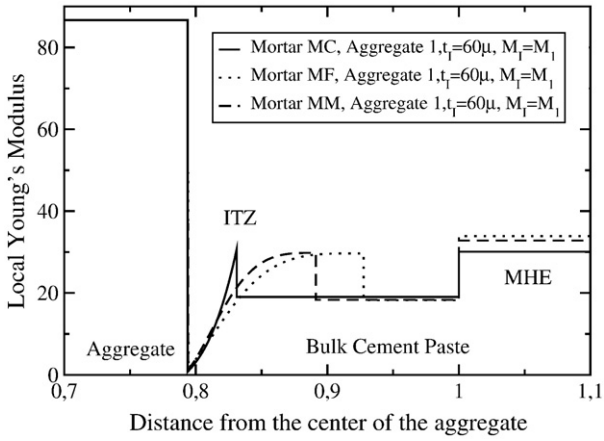

Fig. 12. Local Young's modulus in each phase for different mortars versus the normalized distance from the aggregate.

comparisons between predicted results and experimental ones have been carried out:

- the $(n+1)$-phase model has been adapted to determine the porosity gradient in all inclusion/matrix type composites with interphase (as the ITZ in the case of mortars) from the porosity of the matrix (as the bulk cement paste here), the global porosity and mechanical properties of each phase.
- Microstructural and mechanical properties have been determined on mortars with different sand sizes. Young's modulus of mortars is higher with fine sand (high volume fraction of the ITZ) than with coarse sand (low volume fraction of the ITZ) as a consequence of a lower porosity in the ITZ.
- from the comparison between the experimental and predicted results, by using the $(n+1)$ phase model in an inverse and in direct manner, the following conclusions can be drawn:
  - The possible distribution of porosity (defined by a power-law with an exponent m) within the Interfacial Transition Zone by fitting the model predictions to the measured moduli have been determined. The results show that the exponent m of the power-law depends on the type of sand (size, mechanical properties), on the ITZ characteristics (thickness, composition) and the porosity in the bulk cement paste, and simple values of m (for instance value corresponding to constant, linear or quadratic distribution) are not always possible.
  - The effective Young's modulus may be equal to the experimental average modulus with the same input parameters (sand, thickness and composition of ITZ) for all mortars but the distribution of porosity in cement paste is not the same for small and coarse sands.
  - The tests of different input parameters have shown that the portlandite is always a possible material for the ITZ.

Table 10
Exponent m for the average experimental Young's modulus with the input parameters (A_1, t_2, M_1).

	MF	MM	MC
p_B%			
16.2	2.93	2.50	0.97
17	3.28	2.89	1.31
18	3.2	3.51	1.90
18.2	3.94	3.66	2.05
19	5.51	4.36	2.84
20	5.43	5.58	4.69
22.6	10.3	14.8	No

There is still a need for more experimental results to estimate the Young's modulus in mortars from mixing proportions. This implies a better understanding and a quantification of the characteristics of the Interfacial Transition Zone (composition, gradient) and of the decrease of the bulk cement paste porosity with the size of the sand. This study has to be extended to the case of concrete too.

This micromechanical modeling, taking into account the gradient of properties in cement paste matrix (ITZ and bulk cement paste) allows to study the effect of leaching on mechanical properties. Thanks to the approach presented in this work it will be possible to estimate the evolution of the elastic moduli of mortars subjected to leaching by taking into account the increase of porosity induced by dissolution of portlandite.

Appendix A

Elastic properties of porous materials and of multiply coated particle-reinforced composites

Elastic properties of porous materials

The effective behavior of a composite material made of pores (volume fraction c) embedded in a matrix (let (μm, ν_m, K_m) be respectively its shear modulus, its Poisson's ratio and its bulk modulus) is given by:

$$K^{\text{eff}} = \frac{4\mu_m K_m(1-c)}{4\mu_m + 3K_m c} \tag{14}$$

and the effective shear modulus is the positive root of the following second order equation:

$$A\left(\frac{\mu}{\mu_m}\right)^2 + B\left(\frac{\mu}{\mu_m}\right) + C = 0 \tag{15}$$

with:

$$A = 2(4-5\nu_m)(7+5\nu_m)c^{\frac{10}{3}} - 25\left(\nu_m^m - 7\right)c^{\frac{7}{3}} - 252c^{\frac{5}{3}} + 50(7-12\nu_m + 8\nu_2^m)c + 4(7-10\nu_m)(7-5\nu_m)$$
$$B = -(7+5\nu_m)(1-5\nu_m)c^{\frac{10}{3}} + 50\left(\nu_2^m - 7\right)c^{\frac{7}{3}} + 504c^{\frac{5}{3}} + 150\nu_m(\nu_m - 3)c + 3(15\nu_m - 7)(7-5\nu_m)$$
$$C = (5\nu_m - 7)(7+5\nu_m)c^{\frac{10}{3}} - 25\left(\nu_m^2 - 7\right)c^{\frac{7}{3}} - 252c^{\frac{5}{3}} - 25\left(\nu_m^2 - 7\right)c - (7+5\nu_m)(7-5\nu_m)$$

It is worth noting that the foregoing results (given by Eq. (14) for K by and by Eq. (15) for μ) can also been derived by considering that, in the Generalized-Self-Consistent model proposed by Christensen and Lo [32], the bulk and shear moduli of the innermost phase tend to zero (See Hervé and Pellegrini [33]).

Elastic properties of multiply coated particle-reinforced composite

From Hervé and Zaoui [31] we can determine the effective behavior of multiply coated particle-reinforced composite. Let $\mathbf{N}^{(k)}$ and $\mathbf{M}^{(k)}$ be

$$N^{(k)} = \frac{1}{3K_{k+1} + 4\mu_{k+1}} \begin{pmatrix} 3K_k + 4\mu_{k+1} & \frac{4}{R_k^3}(\mu_{k+1} - \mu_k) \\ 3(K_{k+1} - K_k)R_k^3 & 3K_{k+1} + 4\mu_k \end{pmatrix} \tag{16}$$

and

$$\mathrm{M}^{(k)} = \frac{1}{5(1-\nu_{k+1})} \begin{pmatrix} \frac{c_k}{3} & \frac{R_k^2(3b_k - 7c_k)}{5(1-2\nu_k)} & -\frac{12\alpha_k}{R_k^5} & \frac{4(f_k - 27\alpha_k)}{15(1-2\nu_k)R_k^3} \\ 0 & \frac{(1-2\nu_{k+1})b_k}{7((1-2\nu_k)} & -\frac{20((1-2\nu_{k+1})\alpha_k}{7R_k^7} & -\frac{12\alpha_k(1-2\nu_{k+1})}{7(1-2\nu_k)R_k^5} \\ \frac{R_k^5\alpha_k}{2} & -\frac{R_k^7(2a_k + 147\alpha_k)}{70(1-2\nu_k)} & \frac{d_k}{7} & \frac{R_k^2[105(1-\nu_{k+1}) + 12\alpha_k(7-10\nu_{k+1}) - 7e_k]}{35(1-2\nu_k)} \\ -\frac{5}{6}(1-2\nu_{k+1})\alpha_k R_k^3 & \frac{7(1-2\nu_{k+1})\alpha_k R_k^5}{} & 0 & \frac{e_K(1-2\nu_{k+1})}{3(1-2\nu_k)} \end{pmatrix} \tag{17}$$

with

$$a_k = (7+5\nu_k)(7-10\nu_{k+1})\frac{\mu_k}{\mu_{k+1}} - (7-10\nu_k)(7+5\nu_{k+1})$$
$$b_k = 4(7-10\nu_k) + (7+5\nu_k)\frac{\mu_k}{\mu_{k+1}}$$
$$c_k = (7-5\nu_{k+1}) + 2(4-5\nu_{k+1})\frac{\mu_k}{\mu_{k+1}}$$
$$d_k = (7+5\nu_{k+1}) + 4(7-10\nu_{k+1})\frac{\mu_k}{\mu_{k+1}}$$
$$e_k = 2(4-5\nu_k) + (7-5\nu_k)\frac{\mu_k}{\mu_{k+1}}$$
$$f_k = (4-5\nu_k)(7-5\nu_{k+1}) - (4-5\nu_{k+1})(7-5\nu_k)\frac{\mu_k}{\mu_{k+1}}$$
$$\alpha_k = \frac{\mu_k}{\mu_{k+1}} - 1$$

We now consider the particular matrices:

$$\mathbf{Q}^{(k)} = \prod_{j=k}^{1} \mathbf{N}^{(j)};\ \mathbf{P}^{(k)} = \prod_{j=k}^{1} \mathbf{M}^{(j)} \tag{18}$$

and from $\mathbf{P}^{(k)}$ we can define the matrix $\mathbf{Z}^{(k)}$ by

$$Z_{\alpha\beta} = P_{\alpha 1}^{n-1} P_{\beta 2}^{n-1} - P_{\beta 1}^{n-1} P_{\alpha 2}^{n-1} \text{ with } \alpha \in [1,4] \text{ and } \beta \in [1,4] \tag{19}$$

with $\alpha\in[1,4]$ and $\beta\in[1,4]$.

The effective behavior (K^{eff}, μ^{eff}), respectively the bulk modulus and the shear modulus, of such materials are given by:

$$K^{\text{eff}} = \frac{3K_n R_n^3 Q_{11}^{(n-1)} - 4\mu_n Q_{21}^{(n-1)}}{3\left(R_n^3 Q_{11}^{(n-1)} + Q_{21}^{(n-1)}\right)} \tag{20}$$

and μ^{eff} is the positive root of the following second order equation:

$$A\left(\frac{\mu}{\mu_m}\right)^2 + B\left(\frac{\mu}{\mu_m}\right) + C = 0 \tag{21}$$

with:

$$A = 4R_n^{10}(1-2\nu_n)(7-10\nu_n)Z_{12} + 20R_n^7\left(7-12\nu_n+8\nu_n^2\right)(7-10\nu_n)Z_{42} + 12R_n^5(1-2\nu_n)(Z_{14}-7Z_{23}) + 20R_n^3(1-2\nu_n)^2 Z_{13} + 16(4-5\nu_n)(1-2\nu_n)Z_{43}$$
$$B = 3R_n^{10}(1-2\nu_n)(15\nu_n-7)Z_{12} + 60R_n^7(\nu_n-3)\nu_n Z_{42} - 24R_n^5(1-2\nu_n)(Z_{14}-7Z_{23}) - 40R_n^3(1-2\nu_n)^2 Z_{13} - 8(1-5\nu_n)(1-2\nu_n)Z_{43}$$
$$C = -R_n^{10}(1-2\nu_n)(7+5\nu_n)Z_{12} + 10R_n^7\left(7-\nu_n^2\right)Z_{42} + 12R_n^5(1-2\nu_n)(Z_{14}-7Z_{23}) + 20R_n^3(1-2\nu_n)^2 Z_{13} - 8(7-5\nu_n)(1-2\nu_n)Z_{43}$$

References

[1] R.W. Zimmerman, M.S. King, P.J.M. Monteiro, The elastic moduli of mortar as a porous-granular material, Cem. Concr. Res. 16 (1986) 239–245.
[2] G.T. Kuster, M.N. Toksöz, Velocity and attenuation of seismic waves in two-phase media: Part I, Geophysics 39 (1974) 587–606.
[3] C.C. Yang, R. Yuang, Double inclusion model for approximate elastic moduli oc concrete material, Cem. Concr. Res. 26 (1996) 83–91.
[4] O. Bernard, F.J. Ulm, E. Lemarchand, A multiscale micromechanics-hydration model for the early-age elastic properties of cement-bases materials, Cem. Concr. Res. 33 (2003) 1293–1309.
[5] T. Mori, K. Tanaka, Average stress in matrix and average elastic elastic energy of materials with misfitting inclusion, Acta Metall. 21 (1973) 571–574.
[6] A.U. Nilsen, P.J.M. Monteiro, Concrete: a three-phase material, Cem. Concr. Res. 23 (1) (1993) 147–151.
[7] Z. Hashin, A. Shtrikman, Variational approach to the theory of the elastic behavior of multiphase materials, J. Mech. Phys. Solids 11 (1963) 127–140.
[8] P.K. Mehta, P.J.M. Monteiro, Concrete: Structure, Properties, and Methods, 2nd ed, Prentice-Hall, Englewood Cliffs, N.J, 1993.
[9] S. Mindness, Interfaces in Concrete, Materials sciences of Concrete, in: J.P. Skalny (Ed.), American ceramic Society, Westerville, Ohio, 1989, pp. 163–180.
[10] C.C. Yang, Effect of the transition zone on the elastic moduli of mortar, Cem. Concr. Res. 28 (5) (1998) 727–736.
[11] G. Ramesh, E.D. Sotellino, W.F. Chen, Effect of transition zone on elastic moduli of concrete materials, Cem. Concr. Res. 26 (4) (1996) 611–622.
[12] G. Li, Y. Zhao, S.S. Pang, Four-phase sphere modeling of effective bulk modulus of concrete, Cem. Concr. Res. 29 (1999) 1455–1462.
[13] G. Li, Y. Zhao, S.S. Pang, Y. Li, Effective Young's modulus estimation of concrete, Cem. Concr. Res. 29 (1999) 839–845.
[14] Z. Hashin Test, An inverse method to determine the elastic properties of the interphase between the aggregate and the cement paste, Cem. Concr. Res. 32 (2002) 1291–1300.
[15] Z. Sun, E.J. Garboczi, S.P. Shah, Modeling the elastic properties of concrete composites: experiment, differential effective medium theory and numerical simulation, Cem. Concr. Compos. 29 (2007) 22–38.
[16] M. Lutz, R. Zimmerman, Effect of the interphase zone on the bulk modulus of a particulate composite, J. Appl. Mech. 63 (1996) 855–861.
[17] E. Garboczi, D. Bentz, Analytical formulas for the interfacial transition zone properties, Adv. Cem. Based Mater. 6 (1997) 99–108.
[18] J.C. Nadeau, Water-cement ratio gradients in mortars and corresponding effective elastic properties, Cem. Concr. Res. 32 (2002) 481–490.
[19] J.C. Nadeau, A multiscale model for effective moduli of concrete incorparating ITZ water-cement gradients, aggregate size distributions, and entrapped voids, Cem. Concr. Res. 33 (2003) 103–113.
[20] S. Caré, Aggregate influence on chloride ion diffusion into mortar, Cem. Concr. Res. 33 (2003) 1021–1028.
[21] S. Caré, E. Hervé, Application of n-phase Model to the Diffusion Coefficient of Chloride in Mortar, Transport in Porous Media, Issue 2, August 2004, pp. 119–135.
[22] H.S. Wong, N.R. Buenfeld, Euclidean distance for computing microstructural gradients at interfaces in composites materials, Cem. Concr. Res. 36 (2006) 1091–1097.
[23] J.J.M. Monteiro, P.K. Mehta, Ettringite formation on the aggregate cement paste interface, Cem. Concr. Res. 15 (1985) 378–380.
[24] K.L. Scrivener, Backscattered electron imaging of cementitious microstructures: understanding and quantification, Cem. Concr. Compos. 26 (2004) 935–945.

[25] L. Basheer, P.A.M. Basheer, A.E. Long, Influence of coarse aggregate on the permeation, durability and the microstructure characteristics of ordinary Portland cement concrete, Constr. Build. Mater. 19 (2005) 682–690.
[26] A. Bentur, M.G. Alexander, A review of the work of the Rilem TC 159-ETC. Engineering of the interfacial transition zone in cementitious composites, Mater. Struct. 33 (2000) 82–87.
[27] A. Elshrief, M.C. Cihen, J. Olek, Influence of aggregate size, water cement ratio and age on the microstructure of the interfacial zone, Cem. Concr. Res. 33 (2003) 1837–1849.
[28] S. Diamond, Mercury porosimetry: an inappropriate method for the measurement of pore size distributions in cement-based materials, Cem. Concr. Res. 30 (2000) 1517–1525.
[29] C. Boulay, A. Colson, A concrete extensomater eliminating the influence of transverse strains on the measurement of longitudinal strains, Mater. Struct. 14 (1981) 35–38.
[30] K. Velez, S. Maximilien, D. Damidot, G. Fantozzi, F. Sorrentino, Determination by nanoindentation of elastic modulus and hardness of pure constituents of Portland cement clinker, Cem. Concr. Res. 31 (2001) 555–661.
[31] E. Hervé, A. Zaoui, n-layered inclusion-based micromechanical modelling, Int. J. Eng. Sci. 31 (1) (1993) 1–10.
[32] R.M. Christensen, K.H. Lo, Solutions for effective shear properties in three phase sphere and cylinder models, J. Mech. Phys. Solids 27 (1979) 315–330.
[33] E. Hervé, O. Pellegrini, The elastic constants of a material containing spherical-coated holes, Arch. Mech. 47 (2) (1995) 223–246.